Article:
Loveridge, F orcid.org/0000-0002-6688-6305, Powrie, W and Nicholson, D (2014) Comparison of two different models for pile thermal response test interpretation. Acta Geotechnica, 9 (3). pp. 367-384. ISSN 1861-1125

https://doi.org/10.1007/s11440-014-0306-3

Comparison of Two Different Models for Pile Thermal Response Test Interpretation

Authors:

Dr Fleur Loveridge[1], Prof William Powrie[2] & Duncan Nicholson[3]

1. Corresponding author:
   Lecturer in Geomechanics & Royal Academy of Engineering Research Fellow
   Faculty of Engineering & the Environment, University of Southampton, Highfield, Southampton, SO17 1BJ, fleur.loveridge@soton.ac.uk, 00447773346203.
2. Dean and Professor of Geotechnical Engineering
   Faculty of Engineering & the Environment, University of Southampton, Highfield, Southampton, SO17 1BJ, wp@soton.ac.uk, 00447773346203.
3. Director
   Arup, 13 Fitzroy Street London W1T 4BQ United Kingdom, Duncan.Nicholson@arup.com

Keywords:

Ground source heat pumps; thermal response tests, piled foundations, thermo-active foundations, thermal affects

Symbols used:

Fo	Fourier number ($\alpha t/r_b^2$)
G	G-function
H	pile or borehole length
h_i	heat transfer coefficient
Q	total heating power (W)
q	heating power per unit length (W/m)
R	thermal resistance (mK/W)
R_b	pile thermal resistance (mK/W)
R_c	concrete resistance (mK/W)
R_p	pipe resistance (mK/W)
r	radial position (m)
r_b	pile radius (m)
S_c	specific heat capacity (J/kgK)
S_{cv}	volumetric heat capacity (J/m^3K)
T	temperature (K or C)
ΔT	change in temperature (K or C)
t	time (s)
α	thermal diffusivity (m^2/s)
γ	Euler's constant
λ	thermal conductivity (W/mK)

Subscripts

b	pile or borehole
c	concrete
f	fluid
g	ground
i	inner pipe diameter
in	inlet
o	outer pipe diameter
out	outlet
p	pipe

Comparison of Two Different Models for Pile Thermal Response Test Interpretation

Abstract

Thermal response tests (TRTs) are regularly used to characterise the thermal resistance of borehole heat exchangers and to assess the thermal conductivity of the surrounding ground. It is becoming common to apply the same in situ testing technique to pile heat exchangers, despite international guidance suggesting that TRTs should be limited to hole diameters of 152mm (6 inches). This size restriction arises from the increased thermal inertia of larger diameter heat exchangers, which invalidates the assumption of a steady state within the concrete needed to interpret the test data by traditional line source analysis techniques. However, new methods of analysis for pile heat exchangers have recently been developed that take account of the transient behaviour of the pile concrete. This paper applies these new methods to data from a multi-stage TRT conducted on a small diameter test pile. The thermal conductivity and thermal resistance determined using this method are then compared with those from traditional analytical approaches based on a line source analysis. Differences between the approaches are discussed, along with the observation that the thermal resistance may not be constant over the different test stages.

1 Introduction

Ground energy systems use a heat pump to extract (and/or inject) heat seasonally from the ground beneath or adjacent to a building. Modern ground source heat pumps have a coefficient of performance of around 4 (e.g. [1]) indicating that the heat pump produces four units of heating energy for every unit of electrical energy input. This gives rise to the possibility of significant energy savings over the lifetime of a structure and the prospect of sustainable space heating and cooling solutions. By utilising the building's foundation piles as heat exchangers for the ground energy system rather than just as structural elements, the monetary and carbon costs of a project can be minimised over its lifetime [2-5]. To make dual use of foundations in this way, piles need to be equipped with a number of heat transfer pipes through which a fluid is circulated. This heat transfer fluid also passes through the heat pump. The pipe circuit on the ground side of the heat pump is often referred to as the primary circuit, with the corresponding heat delivery system within the building known as the secondary circuit (**Figure 1**).

Figure 1 Ground Energy System using Pile Heat Exchangers

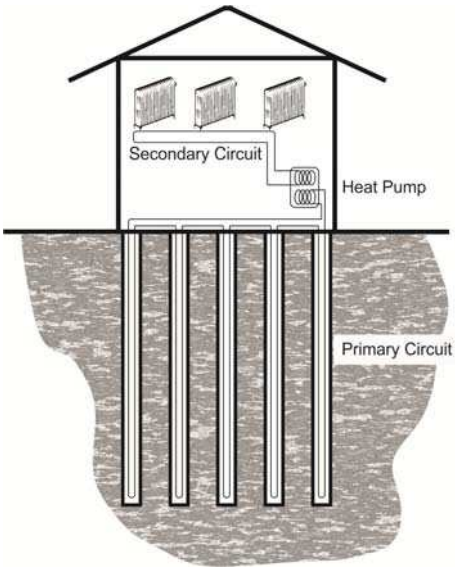

1.1 Pile Heat Exchangers

It is important to understand the differences between pile heat exchangers and more traditional borehole heat exchangers. Systems using boreholes for the primary circuit have been common for many decades, with development of the technology and associated analysis methods led by Northern Europe and North America. The heat exchangers are typically very slender with an aspect ratio (length, H, to diameter, $2r_b$) in the region of 500 to 2000. Borehole diameters rarely exceed 200mm. The slender nature of the heat exchanger means that for much of the soil around the borehole the heat flow is effectively radial. Axial effects caused by the ends of the heat exchanger do occur but these take many years to become significant. Pile heat exchangers by contrast may have a diameter anywhere between 300mm (occasionally smaller) and 1200mm (occasionally larger). Their aspect ratio is typically less than 50 [6] and therefore axial effects can become significant in much shorter time periods.

Another consequence of the larger diameter of pile heat exchangers is that in the short term their thermal behaviour is influenced to a much greater extent by the concrete or grout that forms the heat exchanger. For borehole heat exchangers the heat capacity of the grout is often neglected when evaluating a thermal response tes as under constant thermal power a thermal steady state will be reached in a few hours. For piles however, this process is likely to take much longer [7] and hence to neglect the heat exchanger capacity can lead to an overestimation of the temperature changes in both the heat transfer fluid and the surrounding ground.

1.2 In Situ Characterisation

Design of any ground energy system involves prediction of the temperature changes in the heat transfer fluid and the ground and hence requires knowledge of the key system characteristics. The ground thermal conductivity (λ_g) and the steady state thermal resistance of the heat exchanger (R_b) are two of the most important parameters that directly influence the temperature changes in the primary circuit. In accordance with Fourier's Law, the ground thermal conductivity will control the temperature changes that develop in the ground in response to the heat injected or extracted. The steady state pile thermal resistance then characterises the temperature difference between the heat transfer fluid and the edge of the pile. It is important to be able to predict these temperature changes accurately – firstly to avoid excessive temperatures which can be detrimental to both pile structural performance and heat pump efficiency [8] and secondly to ensure that the maximum energy is obtained from the system [9].

The ground thermal conductivity and heat exchanger thermal resistance are often determined in situ using a thermal response test (TRT). The test was first proposed for use with borehole heat exchangers in 1983 by Mogensen [10] and then further developed in the 1990's [11,12]. Its application for boreholes is therefore well understood [13, 14]. However, the model that underpins normal test interpretation methods assumes that a steady state is rapidly reached within the heat exchanger, allowing the test to be completed within two or three days. For larger diameter piles this will not be the case, hence international guidance restricts the use of TRTs to heat exchangers of 152mm (6 inches) in diameter or less [15]. Using a case study of a multi-stage TRT carried out on a 300m diameter test pile, this paper examines an alternative model which should permit interpretation of the test for larger diameters. In addition, the possibility for different behaviour relating to different tests stages is also explored to determine whether a full picture is being obtained from rapid tests with only a single direction of heat flow.

2 Thermal Response Testing

2.1 Method

Thermal response testing is carried out in situ, usually on a single heat exchanger that forms part of the system primary circuit. The heat exchanger is subjected to heat injection at a constant rate, while the flow rate, fluid inlet and outlet temperatures and ambient air temperatures are measured. The temperature change of the fluid due to the heat injection is then used to calculate the thermal properties. To encourage consistent and rigorous thermal response testing, a number of international and national guidelines are now available [15-17]. The normal test steps are:

1. Purging of air from the pipe circuit by circulating fluid at a high flow rate.
2. Circulation of the heat transfer fluid within the pipe circuit to allow a thermal equilibrium to be established. This allows an indication of the average "undisturbed" ground temperature to be determined.
3. Injection of heat at a constant rate by passing the circulating heat transfer fluid through a heater or a series of heaters for at least 50 hours.

Many TRTs finish after the heat injection step. However, a separate indication of the ground thermal conductivity can be made by continuing monitoring during the thermal recovery:

4. Continue to monitor the fluid temperatures during circulation but with all heaters switched off.

Additional monitoring of thermal recovery has the advantage of not being subject to heating rate fluctuations than can develop during step 3, depending on the source of electricity used for the heaters and whether the surface pipe work is sufficiently insulated to prevent the ambient air temperature from having an influence on the results.

2.2 Interpretation

Most routine TRT interpretation is carried out by a simple analytical technique, based on the so-called line source model (**2.2.1**). However, a number of more sophisticated models are available and these will also be discussed with respect to two different interpretation approaches.

2.2.1 Line Source Model

Assuming an infinite line heat source of constant power per unit depth, q (W/m), the temperature change in the ground, ΔT_g (°C), with time, t (s), can be characterized by the following expression [18]:

Equation 1
$$\Delta T_g = \frac{q}{4\pi\lambda_g}\int_{r^2/4\alpha t}^{\infty}\frac{e^{-u}}{u}du \cong \frac{q}{4\pi\lambda_g}\left(\ln\left(\frac{4\alpha_g t}{r^2}\right)-\gamma\right)$$

where λ_g and α_g are the ground thermal conductivity (W/mK) and diffusivity (m^2/s) respectively, r is the radial coordinate and γ is Euler's Constant. As the heat injection is not applied directly to the ground, but via the heat transfer fluid, the temperature change between the fluid and the edge of the heat exchanger ($r=r_b$) must also be accounted for. This is usually done by assuming a constant steady state thermal resistance for the heat exchanger, so that the temperature change of the fluid is given by:

Equation 2
$$\Delta T_f = qR_b + \frac{q}{4\pi\lambda_g}\left(\ln(4Fo)-\gamma\right)$$

where Fo, is the Fourier number (non-dimensional time), equal to $\alpha_g t/r_b^2$. The non-dimensional expression of the second term in **Equation 2** is given in **Figure 2**. The first term in **Equation 2** gives the inclusion of the thermal resistance term, R_b. This is a lumped term, which includes the effects of the fluid, the pipes and the concrete or grout within the heat exchanger and assumes these regions to all be at a thermal steady state. ΔT_f is the mean temperature change in the fluid and is usually taken to be the average of the inlet and outlet temperatures.

Equation 2 is linear (**Figure 2)** and therefore the gradient of a graph describing the evolution of ΔT_f against the natural logarithm of time can be used to determine the thermal conductivity λ_g. It is also possible to determine the borehole thermal resistance R_b from the intercept, providing an assumption is made regarding the value of volumetric heat capacity, S_{cv} (J/m^3K) used to derive the thermal diffusivity:

Equation 3
$$\alpha = \frac{\lambda}{S_{cv}}$$

Owing to the simplicity of this model it is widely used in practice. However, in part due to the mathematical simplification in **Equation 1**, and in part due to the time it takes the heat exchanger itself to reach a steady state (so that R_b becomes constant), it is important that the early time data from a TRT is neglected. Typically data from $t > 5r_b^2/\alpha_g$ is used in the interpretation. Hellstrom [19] suggests that use of this expression will lead to model fit errors of less than 10%. However, some authors (e.g. [20]) suggest that the criterion should be $t > 20r_b^2/\alpha_g$, which would reduce model fit errors less than 2.5% [19]. An important point is that larger diameter heat exchangers will require a longer period of initial test data to be neglected. However, the errors quoted are model fit errors with respect to the line source assumption (**Equation 1**); they do not include errors resulting from the heat exchanger not having reached steady state, which will take and increasingly longer time with pile diameter [7].

Nonetheless, most authors suggest that for small diameter borehole heat exchangers the TRT in combination with line source model is an appropriate test method (e.g. as used by Banks et al [21]). It tests a larger volume of soil than laboratory methods and gives a lumped value of thermal conductivity of the soils that will be activated by the heat exchanger. Overall accuracies are quoted at 5 to 10% for thermal conductivity and 10 to 15% for thermal resistance [13, 14, 22, 23].

Figure 2 Temperature Changes in the Ground Around a Pile as described by Pile G-functions compared with Infinite Line and Cylindrical Heat Sources

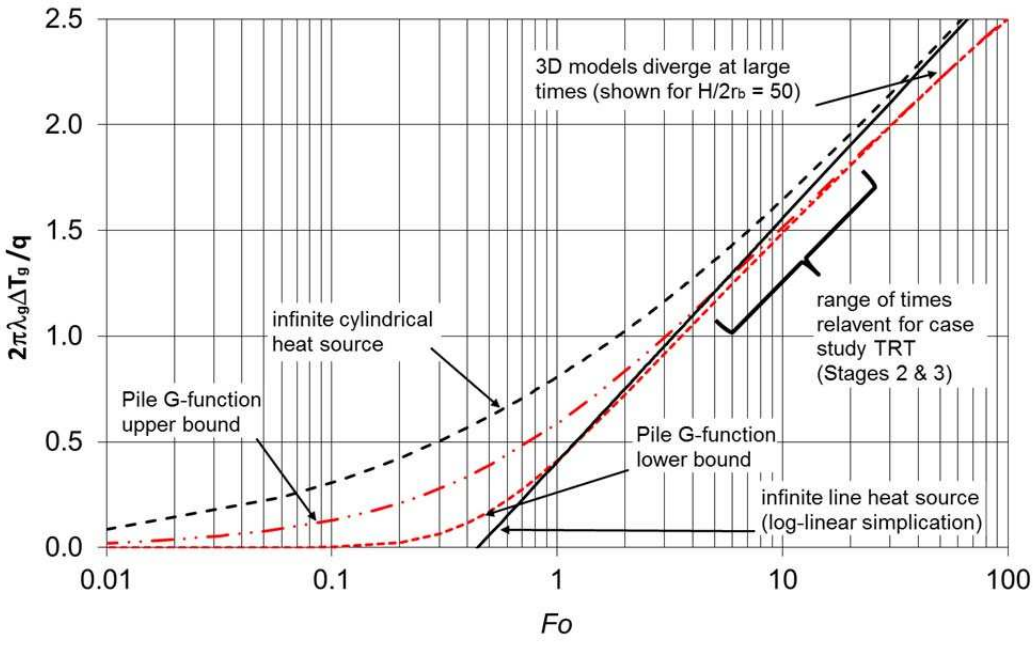

2.2.2 Cylindrical Source Model

Instead of assuming that the heat exchanger acts as a line heat source, it is possible to apply the analytical solution for an infinite hollow cylindrical heat source. The full analytical expression is given by **Equations 4, 5** and **6** [24]:

Equation 4 $$\Delta T_g = \frac{qG}{2\pi\lambda_g}$$

where G is a function of the Fourier number (*Fo*), and r/r_b. G is then given by the expression:

Equation 5 $$G = \frac{2}{\pi}\int_0^{\infty} f(\beta)d\beta$$

where:

Equation 6
$$f(\beta)=\frac{\frac{e^{-(\beta^2 Fo)}-1}{J_1^2(\beta)+Y_1^2(\beta)}\left[J_0\left(r/r_b,\beta\right)Y_1(\beta)-J_1(\beta)Y_0\left(r/r_b,\beta\right)\right]}{\beta^2}$$

Due to the complexities of **Equation 6**, it is more common to apply series expansion solutions for G, such as the one by Bernier [25]:

Equation 7
$$G/(2\pi)=10^{\left[-0.89129+0.36081\log Fo-0.05508\log^2 Fo+0.00359617\log^3 Fo\right]}$$

In both cases an additional term must still be added to account for the heat exchanger resistance as in **Equation 2**.

Even using the simplified **Equation 7**, deriving λ_g and R_b becomes more complicated than when using the line source model. While the log-linear nature of **Equation 2** makes it possible to determine the two variables separately, the cylindrical source equations must be fitted to the test data using a parameter estimation technique. Nonetheless, the approach has been applied by a number of authors [20, 26 - 28]. Both Gehlin and Yu et al compared the cylindrical source to the line source for a number of TRT datasets, finding that the cylindrical source always gave a higher thermal conductivity and thermal resistance by 10% to 15% [20, 28]. This is consistent with the cylindrical source equations calculating higher temperature changes than the line source at short times for the same thermal properties [29], see also **Figure 2**.

2.2.3 Approaches to Power Variation

In both of the models described above it is assumed that the power, q, applied to the heat exchanger is constant. This is sometimes referred to as "direct" application of the model [30]. ASHRAE [31] recommends that for practical purposes constant power means that the standard deviation of the applied power should be less than ±1.5% of the mean and that individual peaks are no more than 10% of the mean. However, if, as is sometimes the case, the power is found to fluctuate more than this then superposition of the applied power can be used during parameter estimation. In its general form:

Equation 8
$$\Delta T_n=\sum_{i=1}^{i=n}\frac{q_i}{2\pi\lambda_g}\left[G\left(Fo_n-Fo_{(i-1)}\right)-G\left(Fo_n-Fo_i\right)\right]$$

where n is the point in time (measured by the Fourier number, *Fo*) at which the superposition is evaluated, *i* is the number of the time-step and G is the function which describes the model being used, which has been calculated at the value of *Fo* prescribed in the equation. It follows from **Equation 2** that for the line source:

Equation 9
$$\boldsymbol{G=(log(4Fo)-\gamma)/2}$$

while for the cylindrical source G is given by **Equation 5** or **Equation 7**. Sauer [32] has recently shown superposition using simple models like the line source to be a very powerful technique for variable power TRTs and for the approach to compare well to finite element models.

2.2.4 Other Interpretation Methods

There are also a number of other interpretation methods for thermal response tests based on either analytical or numerical models. Most of these are applied by parameter estimation techniques using superposition of variable thermal power, but they could equally be applied directly. For example the analytical model of Javed & Claesson [33] has been used for TRT interpretation [30]. The model uses a single equivalent diameter pipe as a substitute for a pair of heat exchanger pipes, which is surrounded concentrically by grout and soil. The model solves for radial heat transfer in the Laplace domain and has the benefit of using the grout thermal properties directly rather than applying a thermal resistance. This means that it can capture non steady behaviour within the

grout. However, it has not been tested for piles so the impact of the pipe simplification on these type of heat exchanger is not yet known.

Perhaps the most commonly applied numerical model is the Geothermal Properties Measurement (GPM) tool [34]. This is a freely available parameter estimation programme developed by Oak Ridge National Laboratory [35]. The tool uses numerical solutions to the one dimensional diffusion equation in radial coordinates to determine the best fit thermal resistance and ground thermal conductivity for TRT data. As the tool is solving the relevant equations directly it is theoretically valid at short time periods when simpler analytical models are known to be unrepresentative (e.g Section 2.2.1). However, as in [33], GPM simplifies the heat exchanger geometry to an equivalent cylinder of grout with an additional film to represent the heat transfer from the fluid. While this approach has been tested with data from borehole heat exchangers it is not known how well it will perform for pile heat exchangers where the volume of concrete within the heat exchanger is much larger. Hemingway & Long [36] have trialled GPM on short duration TRT data from two mini-piles in Ireland with some success. However, the results showed some variability in comparison with other techniques and laboratory data and the applicability of this method to pile heat exchangers is by no means certain.

Austin et al [37] proposed a two dimensional finite volume numerical model for borehole heat exchangers. This can be used for TRT interpretation with parameter estimation methods. The model has the advantage that the actual cross section of the heat exchanger is modelled with the heat transfer pipes simplified to pie-sector shaped elements to avoid complex meshing. The greater flexibility of this model could make it more suitable for application to piles, although both this and GPM cannot account for axial effects in short pile heat exchangers as they are limited to 2D and 1D respectively.

2.3 Application of TRT to Piles

Despite concerns over the validity of the thermal response testing of larger diameter and short length piles, there has been increasing interest in the application of the test method to pile heat exchangers. Theoretically longer duration tests are required for implementation of the line source model with piles as the criterion to discard the early test data depends on the pile diameter. However, as tests get longer, three dimensional effects become important and simple infinite heat source models or other 1D/2D numerical models may no longer be appropriate (**Figure 2**). In addition, at later times the rate of change of the fluid temperature with time is reduced and therefore the results are more susceptible to noise caused by power fluctuations. Finally, long duration tests have financial implications which would limit their uptake for routine applications.

Lennon et al [38] report TRT results for driven piles less than 300mm in diameter; a successful test of a 300mm diameter bored pile was carried out at the research site described by Wood et al [39]. There are some initial data suggesting successful tests on piles up to 450mm diameter [40, 41]. However, more recent analysis gives an indication that there may be a loss of accuracy with short duration tests on piles of this size [42]. In addition, recent longer duration tests on a 600mm diameter pile gave very variable results [43]. These inconsistent results underline the fact that there has been no rigorous consideration of the method of analysis for pile TRTs. A better understanding of appropriate analysis models and approaches is therefore essential to improve the assessment and design of pile heat exchanger projects.

New empirical models, called G-functions, to simulate the thermal behaviour of pile heat exchangers have recently been proposed [9] and it is planned to use these to analyse thermal response test data. To better capture the pile behaviour a Pile G-function is used to simulate the temperature changes in the ground and a Concrete G-function is used to determine the temperature change between the heat transfer fluid and the ground:

- The Pile G-functions have been developed for typical pile heat exchanger geometries and the calculated temperature response for the pile is between that of a line and cylindrical heat sources in the short term (**Figure 2**). However, the response soon diverges from the infinite heat source models owing to three dimensional effects, for example see **Figure 2**. Importantly, the analysis does not rely on a minimum time period having elapsed, and consequently all the test data may be used in the interpretation.

- The Concrete G-function, which describes the temperature change between the fluid and the pile edge, accounts for the short term storage of heat within the pile concrete. Therefore the validity of the analysis does not depend on the heat exchanger having reached a thermal steady state.

To predict the total temperature change of the fluid, the Pile G-function (temperature change in the ground) and the Concrete G-function (temperature change across the concrete) are summed with the temperature change across the fluid and pipes determined from the pipe resistance, $R_{p,}$ being added separately. This paper will test the application of these new functions to a multi-stage TRT carried out on a 300mm test pile, a full description of the method being given in Section 4.2.

3 Test Details

A 300mm diameter test pile was constructed at a central London development site. The pile hole was bored to 200mm diameter using cable tool methods as part of a ground investigation programme and then reamed out to the larger diameter over the upper 26.8m depth. A single U-loop of heat transfer pipe was then installed in the hole to 26m depth and the hole was backfilled with C35 hard pile cementitious grout designed to mimic the performance of pile concrete. The pipes were made from high performance polyethelene "PE100" material with an external diameter of 32mm and a wall thickness of 2.9mm. The pipes were installed separated by rigid spacers ensuring an even separation of the pipes and a centre to centre spacing between the two legs of the U-tube of around 135mm (**Figure 3**). Below a concrete slab, the "pile" was constructed through London Clay over its entire length. The stratum was described as firm to stiff grey clay and contained layers of claystones at a number of locations. Index test data for the London Clay over the the pile depth are shown in **Figure 4** for samples taken from the pile hole (BH12) and the two nearest other boreholes. Vibrating wire piezometers installed during the ground investigation programme and monitored during the summer and following autumn showed the ground water level at the site to be within 4m of the pile head. It is therefore to be expected that the majority of the soil surrounding the pile is fully saturated.

Figure 3 Pile Geometry

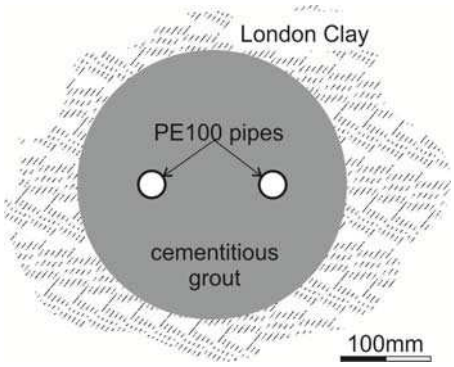

Ten days after grouting the pile a thermal response test was carried out on the pile loop. Measurements were made of flow rate and temperature at five minute intervals using an electromagnetic flow meter and Iron-Constantan (J type) thermocouples respectively. The flow meter has an accuracy of approximately 1% at the flow rates used and a repeatability of ±0.2%. Calibration of the thermocouples prior to the test showed an accuracy within 0.2°C. The circulating fluid used during the tests was water.

The test comprised a number of different stages (**Table 1**). After an initial circulation, a heat injection test and recovery period was followed by a heat extraction test and recovery period. Cyclic testing was then commenced comprising two heat injection stages separated by heat extraction stages. Each test stage followed directly from the preceding stage and the fluid circulation was maintained throughout, except for a 4 day period in stage 6

when shut down was required in order to repair a faulty heating unit in the TRT rig. The output data from the test is shown in Figure 5.

Figure 4 London Clay Moisture Content (Solid Symbols), Plastic Limit (Simple Cross) and Liquid Limit (Complex Cross)

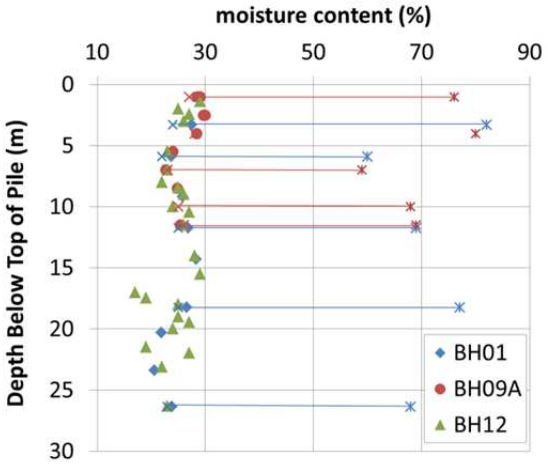

Table 1 Thermal Response Test Stages

Stage	Type	Approximate Duration	Nominal Power Applied	Actual Average Power (Equation 10)	Comments
1	Circulation only	4.5 days	None	-0.067 kW	
2	Heat Injection	3 days	2 kW	2.235 kW	
3	Recovery	3 days	None	-0.091 kW	
4	Heat Extraction	3 days	-2 kW	-2.077 kW	
5	Recovery	4 days	None	0.020 kW	
6	Heat Injection	4 days	None	0.036 kW	Heater faulty
		4 days	None	N/A	No circulation during repairs
		2 days	1.9 kW	1.839 kW	
7	Heat Extraction	2 days	-1.3 kW	-0.739 kW	
8	Heat Injection	2 days	2.1 kW	2.139 kW	
9	Heat Extraction	3 days	-0.8 kW	-0.326 kW	

The nominal heater or chiller power during the various stages of the test is not the most accurate measure of the actual power supplied to the heat exchanger. Consequently the actual applied power, *Q (W)*, was calculated using the inlet to outlet temperature difference, the fluid mass flow rate, $\dot{m}$ (kg/s), and the fluid specific heat capacity, S_c (J/kgK) as follows:

Equation 10 $$\boldsymbol{Q = S_c \dot{m}(T_{out} - T_{in})}$$

Figure 5 plots the actual applied power, Q, and the mean fluid temperature, $[T_{out} + T_{in}]/2$, for all the test stages. Although the applied power is nominally constant during each stage of the test, there are actually significant variations with time, especially during the latter stages of the test. Thus it would be inappropriate to carry out direct analysis of the data for these stages and superposition analysis must be used instead (see also Section 4).

Consideration of the surrounding ambient air temperature (**Figure 5**) appears to show no clear link between these daily temperature fluctuations and the power applied. This suggests that the power fluctuations relate to an instability of supply rather than insufficient test insulation. However, when no power is applied in stage 1 it is possible to see some small influence of the ambient conditions on the mean fluid temperature. The average value during this period indicates the undisturbed ground temperature to be approximately 17.7°C.

Figure 5 Average Fluid Temperature and Applied Thermal Power during the Test

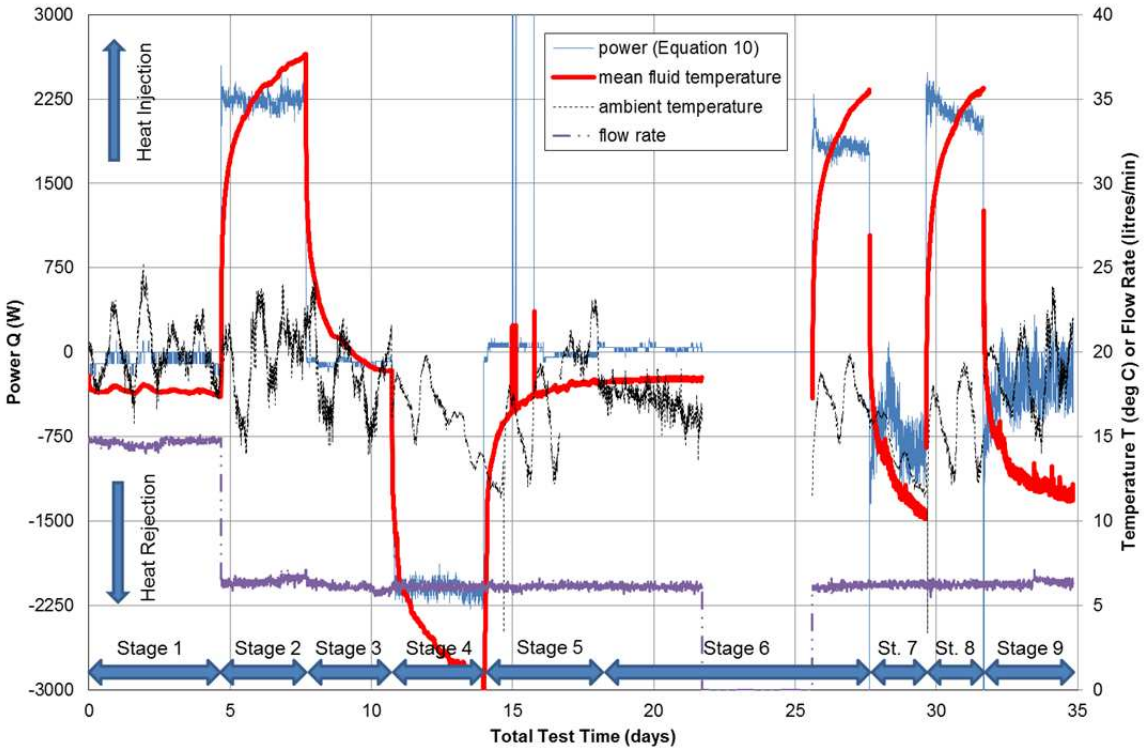

4 Analysis Methods

Two different models were used to interpret the thermal response test data: the line source, as routinely used in practice; and the new pile and concrete G-functions (described in 4.2 below) which have been developed specifically for use with pile heat exchangers. Where possible the two models were used directly assuming constant thermal power. However, practically, this was restricted to Stages 2 and 3 of the test as full recovery to the original "undisturbed" ground temperature was not attained at the end of Stage 3 (**Figure 5**). Previous work has shown that if a repeat TRT is carried out on a borehole where the second starting temperature is 1.1° above the original test then up to 12% variance in the calculated thermal parameters can occur [44]. This led to a recommendation of repeat tests not being carried out until the fluid temperature has returned to within 0.3° of the initial value. The length of time taken for this to occur can depend on the heat injection rate as well as the heating time and ground properties [45]. In any case, it is clear that the fluid temperature at the end of Stage 3 never returned to that at the start of Stage 1 before commencement of the heat rejection of Stage 4. While the recovery period was longer following Stages 4 and 5, the fluid temperature was still 0.4°C below its initial value at the commencement of heat injection during Stage 6. It can also be seen in **Figure 5** that the applied power in the later stages of the test is highly variable and not suitable for direct analysis. Consequently, to permit analysis of all the test data, superposition has also been applied using the line source and G-function models using **Equation 8**.

4.1 Line Source

Equation 2 has been applied to directly to determine λ_g for Stage 2 based on the gradient of the graph of log time vs average fluid temperature. Test data for $t < 5r_b^2/\alpha_g$ has been discarded (assuming S_{cv} for the ground to

be 2.15x10^6 J/m^{3}K). This equates to around 27 hours. Exclusion of more data than this was not found to increase the accuracy of the results as at later test times the noise superimposed on the temperature measurements becomes larger relative to the rate of temperature change. R_b was determined from the straight line intercept, making the same assumption about the volumetric specific heat. The average actual applied thermal power during each test stage was used (**Table 1**).

For direct interpretation of the recovery stage (Stage 3) a similar approach to that used in groundwater pumping tests was applied. By superposition (based on **Equation** 8) it can be shown that the average fluid temperature during the recovery stage is given by:

Equation 11 $$\Delta T_f = \frac{q}{4\pi\lambda_g} \ln\left(\frac{t}{t'}\right)$$

Where t is the length of time elapsed since start of the heat injection and t' is the length of time elapsed since the start of the recovery stage. q is the average power (W/m) applied during the preceding heating stage. As with **Equation 2**, it is possible to determine λ_g directly from the gradient of a log-linear graph. As **Equation 11** also depends on the line source model, the early time (in terms of t') data must similarly be discarded as described above. Note that it is not possible to determine the thermal resistance from the recovery data.

In all cases the values of λ_g and R_b determined were crossed checked by inserting them back into **Equation 2** or **Equation 11** and confirming that the root mean square error was minimised when comparing the calculated temperatures with the values measured during the test.

4.2 Pile and Concrete G-functions

Pile G-functions describe the temperature change of the ground around the heat exchanger, while concrete G-functions describe the temperature change across the concrete pile. The expressions are a function of the applied heating power and the Fourier number (non-dimensional time), *Fo*. Summing the G-functions and the temperature change across the pipe and fluid gives the temperature change of the fluid during heat injection or rejection as follows [9]:

Equation 12 $$\Delta T_f = qR_p + qR_cG_c + \frac{q}{2\pi\lambda_g}G_g$$

where R_p is the resistance of the pipes in the heat exchanger, R_c is the resistance of the concrete part of the pile, G_c is the concrete G-function and G_g is the pile G-function. To determine λ_g and R_c using **Equation 12** the first step is to determine R_p from the following expressions:

Equation 13 $$R_p = R_{pconv} + R_{pcond}$$

where

Equation 14 $$R_{p_{conv}} = \frac{1}{2n\pi r_i h_i}$$

and

Equation 15 $$R_{p_{cond}} = \frac{\ln(r_o/r_i)}{2n\pi\lambda_{pipe}}$$

where n is the number of pipes within the heat exchanger cross section, r_i is the pipe internal radius, r_o is the pipe external radius, λ_{pipe} is the pipe thermal conductivity and h_i is the heat transfer coefficient. The latter can be calculated using the Gnielinksi correlation [46] assuming turbulent flow. For the case under consideration R_p is calculated to be 0.05 mK/W.

The two G-functions take the form of **Equation 16**, where the constants *a* to *h* are dependent on the geometry of the pile, both in terms of the pipe positions and the aspect ratio, $AR=H/2r_b$. Based on the criteria in [9], the values of the constants *a* to *h* used in the analysis are given in **Table 2**. The Pile G-function used in this case, which is a lower bound solution, is plotted in **Figure 2**.

Equation 16

$$G = a[\ln(Fo)]^7 + b[\ln(Fo)]^6 + c[\ln(Fo)]^5 + d[\ln(Fo)]^4 + e[\ln(Fo)]^3 + f[\ln(Fo)]^2 + g[\ln(Fo)] + h$$

Table 2 Values of the Empirical Constants used with the Pile and Concrete G-functions

Empirical Constant	Pile G-function (lower bound, AR≥50)[1]	Concrete G-function (lower bound for pipes near the pile edge)[2]
a	-8.741×10^{-8}	0
b	8.243×10^{-6}	-1.438×10^{-5}
c	-1.835×10^{-4}	1.276×10^{-5}
d	1.894×10^{-3}	9.534×10^{-4}
e	-0.01375	1.307×10^{-4}
f	0.04905	-0.02446
g	0.3997	0.07569
h	0.4267	0.921

Notes: (1) For Fo<0.25 then G=0; (2) For Fo<0.01 G=0 and for Fo>10 G=1

For Stages 2 & 3 where the G-functions could be applied directly, the average power from **Table 1** was applied. Neither unknown variable, λ_g or R_c, can be determined independently so two variable parameter estimation must be carried out. This was done using the SOLVER function in MS Excel. For Stage 3 there is no equivalent simple expression such as **Equation 11**. Consequently **Equation 8** must be applied for n=2 heating steps with $q_{(Stage\ 2)}$ equal to the mean heating power in Stage 2 and $q_{(Stage\ 3)}$ equal to zero.

4.3 Variable Power Superposition

Full application of **Equation 8** with both models allows the power input to be varied over any time increment. In this analysis an interval of 5 minutes was adopted based on the data gathered and to allow the full impact of power variation later in the test to be accounted for. This involves computation of a large summation, hence **Equation 8** was coded in the software MATLAB to minimise the time taken. To reduce the number of iterations required for parameter estimation, values of λ_g and R_c were stepped in intervals of 0.1 W/mK and 0.0125 mK/W respectively. These equate to around 4% and 10% of the expected values. Larger intervals were used for the thermal resistance as it was expected to be able to determine this parameter to a lower level of accuracy [14, 22].

5 Results

5.1 Direct Determination

Table 3 summarises the thermal conductivity and thermal resistance values determined from the thermal response test data using the line source model and the G-functions with a constant applied power (**Table 1**). Where a line source method has been used the thermal resistance calculated is R_b; where the G-functions have been used then the analysis provides a value of R_c and $R_p=0.05$ mK/W must be added to give a comparable total resistance. A measure of the "goodness of fit" is provided in all cases by the root mean square error (RMSE) of the residuals.

For Stage 2 of the test the two models give similar results with a 4% difference in thermal conductivity and only a small difference in thermal resistance. λ_g is lower in the G-function analysis. This is consistent with **Figure 2**, which shows the line source plotting above the pile G-function (for the same thermal properties) for the time period relevant to the test. It shold be noted that although the pile G functions plot between the line and cylindrical sources at very small values of Fo (<1), by Fo=10 three dimensional axial effects mean that the G-

functions are always below the infinite heat source solution. Therefore in back analysis the line source equations would require specification of lower R_b and/or higher λ_g values to output the same temperatures as the G-function.

Table 3 Thermal Conductivity and Thermal Resistance Values Derived from Direct Determination

Test Stage	Model	λ_g	R_c	R_b	RMSE
2	Line Source	2.5		0.123	0.14
	G-function	2.4	0.075	0.125	0.14
3	Line Source	2.7			0.46
	G-function	2.9	0.160	0.210	0.14

Theoretically the G-functions should provide a better fit to the measured data. But, interestingly, the value of the residuals and RMSE are similar for the two models. This is surprising as the G-functions should better represent the actual physical conditions in the ground. The explanation for this result may lie with several factors. First the log-linear simplification of the line source is actually negative at small values of time (**Figure 2**). When the additional temperature change for qR_b is added to this, the resulting temperature changes become positive again and happen to align well with the measured temperatures (**Figure 6**), even though the model is clearly incorrect. In fact, **Figure 6** shows a better short time (<2 hour) fit than the G-function model, which initially overestimates the temperature change. For the G-function model this initial overestimation may reflect transient behaviour within the fluid and the pipes. As the heat exchanger has only two pipes in this case, qR_p is calculated to be as much as 4°C for Stage 2 (**Figure 6**). This temperature change will in reality not occur instantaneously as assumed in the model.

Figure 6 Direct Fit of Line Source and G-function Models to Test Stage 2

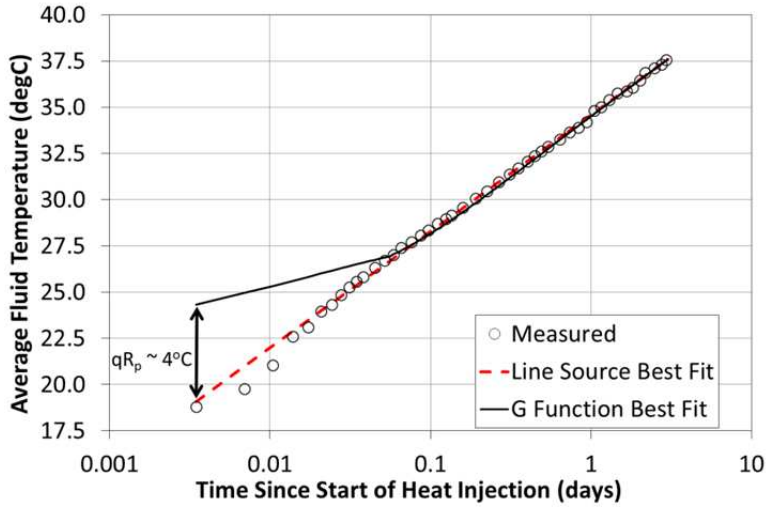

Finally, the close fit of the line source model may also indicate that the grout conductivity and diffusivity are nearly equal to those of the surrounding ground. This would tend to make the real physical scenario closer to the idealised line source model. This hypothesis can be tested by taking the value of R_b determined from the line source model (0.123mK/W) and using this to back calculate λ_c, based on the simplified (2 pipe) first order multipole equation presented in [19]. This approach has been shown to be appropriate for determining 2D pile resistance by comparison with numerical studies [7]. For λ_g=2.5W/mK this analysis shows that λ_c would be 2.55W/mK. The thermal diffusivity of the grout cannot be determined, but based on the densities of these materials these values would be expected to be similar. Nevertheless the fit of the line source model at such small times is still surprisingly good.

Both the line source and G-function models give a larger value of thermal conductivity when fitted to the Stage 3 recovery data (**Table 3**). For the line source model it is not possible to determine a thermal resistance, while for the G-function model the value determined was substantially and possibly unrealistically higher than that

determined in Stage 2 (**Table 3**). While the shapes of the curves were fairly well matched in Stage 2 (**Figure 6**), there is some nonlinearity in Stage 3 which cannot be reproduced by the line source model (**Figure 7**). A better fit was achieved using the G-function model, as reflected in a lower RMSE than the line source model during this stage of the test. As will be seen in the following sections the differences between values of λ_g and R_c determined during Stage 3 and Stage 2 may relate to the applied power not being truly zero during recovery. This will be discussed further in Section 5.2.1.

Figure 7 Direct Fit of Line Source and G-function Models to Test Stage 3

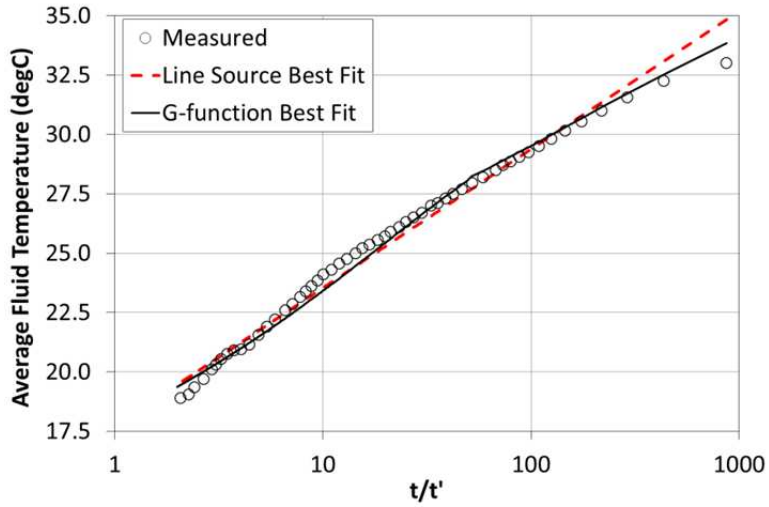

5.2 Variable Power Parameter Estimation

Applying variable power superposition on the basis of **Equation 8** allows all stages of the test data to be back analysed to determine λ_g and R_b. For this exercise the test data has been bundled into four sections: Stage 2 alone, Stages 2 and 3 together, Stages 2 to 5 and Stages 2 to 9. The results of the parameter estimation for these sections are given in **Table 4**.

Table 4 Thermal Conductivity and Thermal Resistance Values Derived from Power Superposition

Test Stage	Method	λ_g	R_c	R_b	RMSE
2	Line Source	2.6		0.125	0.20
	G-function	2.4	0.075	0.125	0.36
2&3	Line Source	2.5		0.125	0.26
	G-function	2.3	0.075	0.125	0.32
2 to 5	Line Source	2.7		0.125	0.92
	G-function	2.6	0.075	0.125	0.97
2 to 9	Line Source	3.2		0.1375	1.87
	G-function	3.15	0.0875	0.1375	1.90

5.2.1 Stages 2 & 3: First Heat Injection & Recovery

When Stage 2 alone is analysed by power superposition the results are similar to the direct application of the two models. The thermal conductivity calculated using the line source model is slightly higher (2.6 W/mK compared with 2.4 W/mK), but otherwise the best fit parameters are very similar. In fact for the G-functions the results are identical. The line source model still provides a surprisingly good fit to the measured data at very small times (**Figure 8**), although RMSE values are slightly higher than for direct application of the models.

When Stages 2 and 3 are analysed together, lower values of thermal conductivity are obtained than with direct model application. These results appear more plausible (λ_g =2.5 W/mK and λ_g =2.3 W/mK for the line source and G-functions respectively) than with direct application ((λ_g =2.7 W/mK and λ_g =2.9 W/mK respectively), which could not fit the observed non linearity in Stage 3. Therefore it is not surprising that the variable power

superposition curves provide a much better fit during Stage 3. This is illustrated in **Figures 9a** and **9b** which are plotted in the same manner as Figures 7 and 8 for direct comparison.

Figure 8 Superposition Fit of Line Source and G-function Models to Test Stage 2 Only

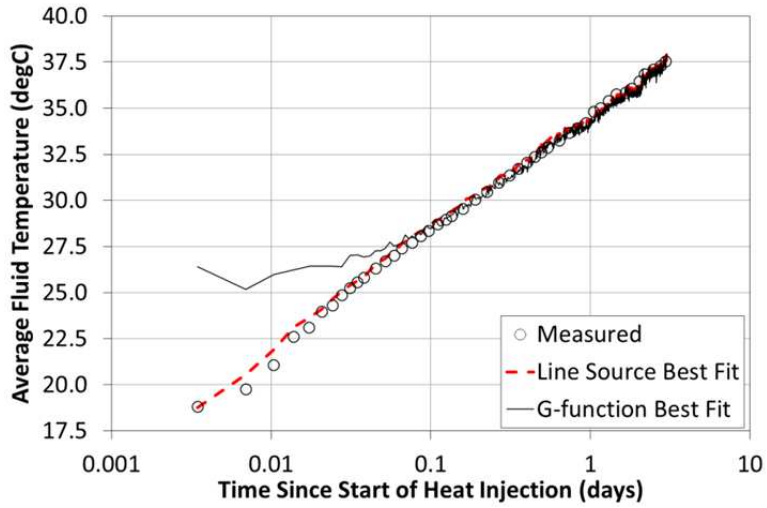

Figure 9 Superposition Fit of Line Source and G-function Models to Stages 2 & 3 Together a) Test Stage 2 & b) Test Stage 3

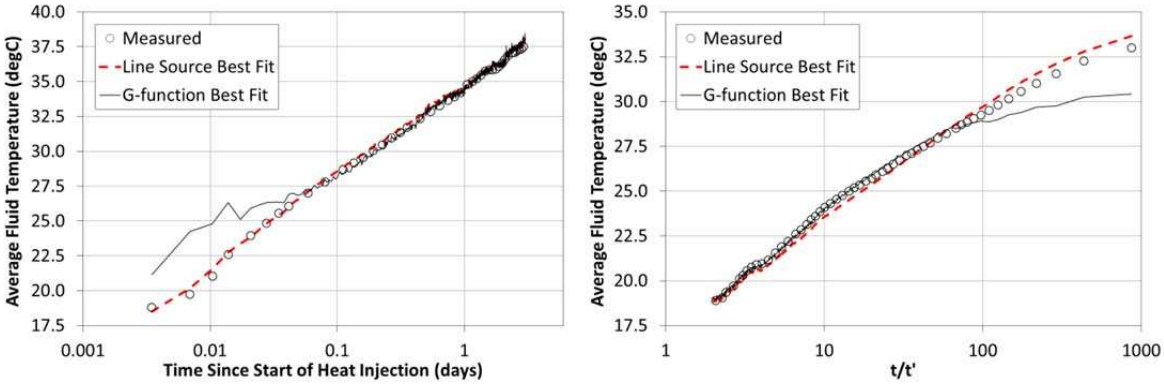

The poorer fit for Stage 3 with direct application of the two models likely reflects the assumption of zero power in that stage, meaning any power input from the circulation pump or outside influences is not accounted for in the model. So, although using the recovery data is in theory more accurate, it is not without additional sources of error as can be seen in this case. On the other hand, when the power superposition approach is used to interpret the recovery data (also including the preceding Stage 2), the shape of the recovery curves is much better represented (**Figure 9**). This demonstrates the ability of the superposition approach to include any small amount of heat input to the system during the recovery process. Overall this approach, using a variable power input, allows a more consistent fit to all the data in the first two stages.

Figures 8 and **9** also show that the superposition approach leads to curves which have greater short term variability that the measured data. While this approach undoubtedly leads to a better fit of the medium to long term power fluctuations, both the line source and G-function models are over predicting the transfer of short term power fluctuations to the heat exchanger. There is clearly some additional buffering in the fluid and pipes that is not being represented by either model.

5.2.2 Stages 2 to 5: Heat Injection & Recovery followed by Heat Extraction & Recovery

When the superposition analysis is extended to include Stages 4 and 5 of the TRT the value of thermal conductivity determined by the two models increases (**Table 4**). The derived resistance values remain similar, but the RMSE is increased to almost 1. As the test progresses the fit of the models to the measured data appears

to be reduced (**Figure 10**). It can also be seen in **Figure 10** that at the end of Stage 4 as the chillers are switched off there is a downward temperature spike. This occurs as the outlet temperature (lower than the inlet temperature in heat injection) increases to match the inlet temperature despite there being no additional input of thermal power. There is no clear reason for this step change, but it may in part explain the reduction in fit quality for the subsequent recovery stage. More positively the temperature spikes measured during Stage 6 due to short lived power surges have been reflected in the fitted curves fit (**Figure 10**), demonstrating the benefits of a variable power superposition approach. However, as observed previously, the damping of short term power fluctuations is not fully captured with the models showing larger temperature changes at the power surges than the measured temperature data.

Figure 10 Superposition Fit of Line Source and G-function Models to Test Stages 2 to 5

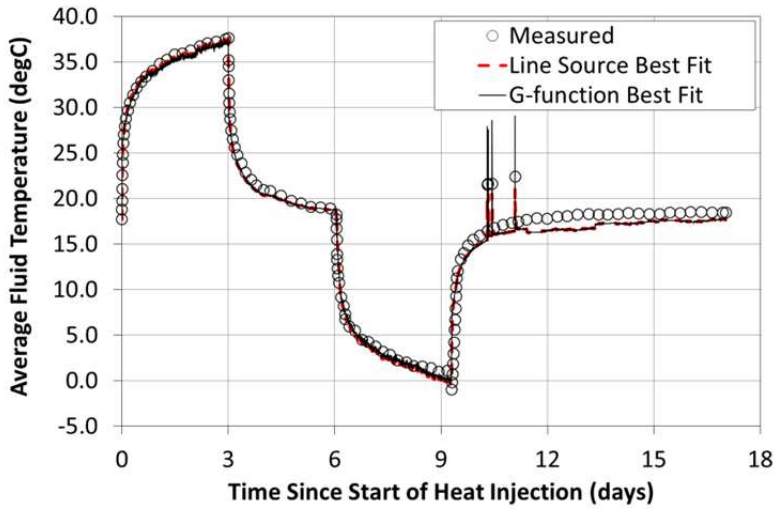

Figure 11 Superposition Fit of Line Source and G-function Models to All Test Stages

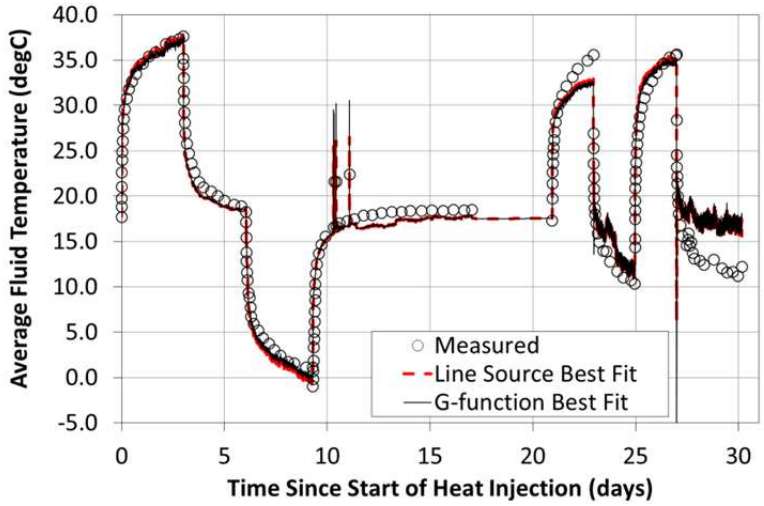

5.2.3 All Test Stages

When all test stages are included in the superposition analysis the derived value of thermal conductivity increases again to 3.2 and 3.15 W/mK for the line source and G-function models respectively (**Table 4**). In this case the derived resistance values also increases and the RMSE is now almost 2, reflecting the poor overall fit shown in **Figure 11**. As in **Figure 10**, the closeness of the fit seems to reduce as the test progresses, with errors approaching 5°C in the final cyclic test stages. In particular there is a trend to under-predict the temperature changes in the cyclic stages of the test and this effect is more pronounced during the stages where the pile is cooled. This deterioration in fit is surprising as superposition of thermal power is a well-established technique

for the analysis of analysis of ground heat exchangers and has been used in the successful back analysis of field data on a number of previous occasions (e.g. [47, 48]). This will be discussed further in Section 6.2.

6 Discussion

6.1 Analysis Method & Approach

An important question is what this thermal response test can tell us about recommended analysis methods, both in terms of the underlying model and method of approach. With respect to the model, the first key observation is that on a single stage basis the line source provides a good fit to the measured data (**Figures 6 & 8**), despite the model not being correct. This is surprising as the G-functions are theoretically a better representation of real pile behaviour. However, it must also be stressed that the log-linear nature of **Figures 6** to **9** do overestimate the importance of the early time data, and in fact the overall fit of the two models in terms of RMSE is similar. In addition, from **Figure 2** it can be seen that axial effects to play a part in the temperature response, even over the duration of a thermal response test. This explains why the line source model consistently gives higher thermal conductivities for the soil than the G-functions. Therefore, while the line source appears to give a good fit, it is expected that it would consistently overestimate the thermal conductivity; in this case by 5% to 10%. It is also important to add that in this case the pile diameter was still relatively small; the line source would be expected to perform less well for larger diameter piles [29, 42] or those with a lesser aspect ratio where axial effects would be more important.

With respect to the analysis approach, direct application of the models gave similar results to power superposition when considered over just the first test Stage. However, both models appear too sensitive to smaller fluctuations in the applied power and that in reality some damping of the temperature response occurs in the heat transfer pipes and fluid system. Nonetheless the power superposition approach is clearly superior when there are more significant medium term power fluctuations which will lead to errors when using the average power approach. It also should be noted that the smaller fluctuations in applied power would also become less significant with larger energy piles having more pipes installed as this would substantially reduce the value of qR_p (**Equations 13** to **15**).

The superposition approach appeared to be better than direct application was when interpreting recovery data. For the line source, the absence of the qR_b term in **Equation 11** means that the model is forced through the origin, when potentially there may still be some power applied due to the operation of the circulation pump, and/or due to other external influences. Recovery data are traditionally viewed as more reliable than heat injection data due to the absence of power supply variations and the fact that λ_g can be determined independently of R_b [49]. However, it comes with the disadvantage of increased test costs. This case study is also showing that it is not necessarily more accurate if the data analysis is restricted to direct application of line source model. Of course, power superposition also allows the full test data to be analysed in this case, although this raises some questions as will be discussed in Section 6.2.

It is also worth observing the co-linear nature of λ_g and R_b when determined from parameter estimation techniques (**Figure 12**) as is required with the G-functions approach. The same is also true for the line source, but because of the log-linear nature of the equation it is possible to determine one parameter independently during direct application, thus reducing the computation effort involved in the analysis. This is a significant practical advantage of the line source, which makes it attractive for use with small diameter heat exchangers.

Overall it must be concluded that for a single stage test on a 300mm diameter pile the line source can be used, as long as it is accepted that there may be some over estimation of the thermal conductivity. In this respect the analysis would not be conservative. Consequently it would be better to fit the G-function models to the test data, which is not considerably more time consuming when using the readily available SOLVER function in MS Excel. The more complex and time consuming application of the models using power superposition does not necessarily offer significant benefit for single stage tests, where the power supply is stable. However, there are

clearly benefits to this approach for analysis of recovery curves, more complex multistage tests or those were the power supply is not stable.

Figure 12 Contours of Route Mean Square Error from Direct Analysis Approach during Stage 2: a) Line Source; b) G-functions

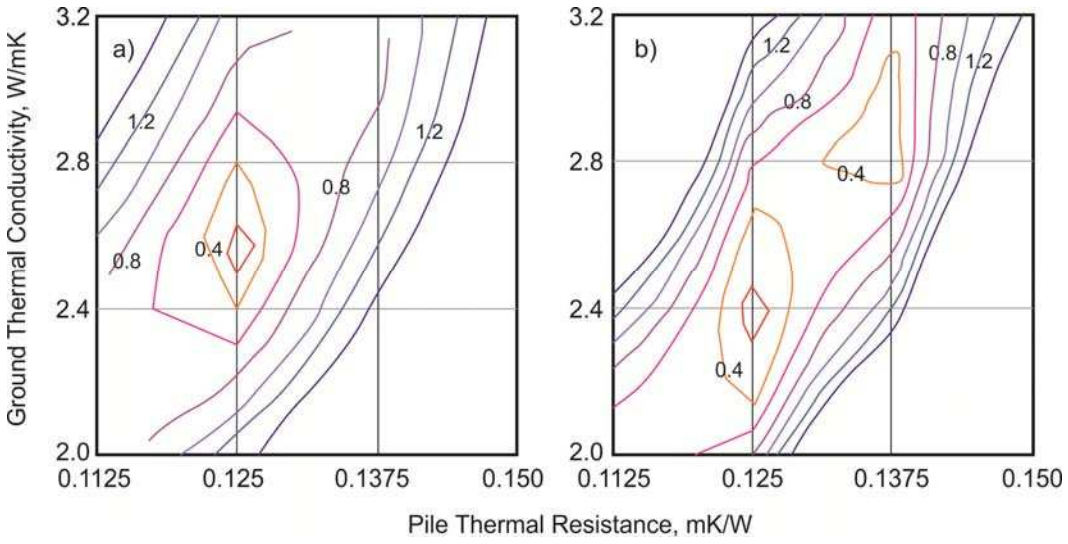

6.2 Heating and Cooling Hysteresis

Figure 11 suggests that the behaviour of the system formed by the pile heat exchanger and the surrounding ground is more complex than is captured by existing models. One possible explanation, given the tendency for poor fit during the later heat extraction stages (**Table 4, Figure 11**), is that the system may be undergoing some sort of hysteresis. It is also possible that this first starts to occur during Stages 4 and 5.

Any hysteresis would be indicative of a change in the effective system characteristics between the different stages. However, soil thermal conductivity should not change by the amount indicated in **Table 4** during the course of the test, being a basic physical property which is controlled by the mineralogy, structure and water content of the soil. While it may be possible in unsaturated soils for water contents to change under thermal gradients and thus affect the thermal conductivity, the ground is saturated in this case and thus changes in water content would not be expected.

Pile thermal resistance on the other hand is a lumped parameter and could conceivably change during the course of the test. First, the resistance is dependent on the flow conditions. Although these are fairly constant throughout the test, and R_{pconv} is less than 0.01 mK/W and thus has only a minor bearing on the total resistance. Secondly, it must be considered that the pile interfaces may change due to the heating/cooling cycles. Taking the data in **Figure 11**, to provide a better fit R_b would need to be larger during heat extraction (as the pile cools) and smaller during heat injection (as the pile is heated). This would be consistent with an increased contact resistance at the pile-soil boundary (or the pipe-grout boundary) if the pile (and/or pipes) contract when cooled. For simplicity contact resistances are not usually accounted for when calculating pile thermal resistance, although in reality the contact of any two surfaces will never be perfect.

Table 5 summarises the results of a best fit analysis in which the thermal conductivity was kept constant but the pile resistance (R_c) varied for each stage of the test. The value of λ_g used was that for Stage 2 of the test given in **Table 4**. The value of R_p used was also kept constant at 0.05 mK/W as per previus analyses. For the case of the line source model, $qR_b = qR_{c+} qR_p$ is a steady term and therefore not subject to superposition. Hence SOLVER can be used to determine the corresponding value of R_c which would give the lowest RMSE for each subsequent stage. For the G-function model (**Equation 12**) the term qR_cG is transient and hence parameter estimation using superposition must be carried out to determine R_c for each test stage. In this case R_c was stepped in finer intervals of 0.00625 mK/W. The results show that the best fit R_c varies considerably over the test. In particular, the latter two stages where the pile is cooled by heat extraction (Stages 7 and 9) show marked

increases in R_c. The initial heat extraction stage (Stage 4) does not show this effect, although it is at this point that the model fit first starts to diverge from the measured data.

Even with a variable R_c, there continues to be a reduction in fit quality throughout the test as evidenced by the increasing values of RMSE (**Table 5**) and the plot in **Figure 13**. However, overall the fit is improved compared to **Figure 11**. The average value of RMSE for all the stages is now 1.17 and 1.16 for the line source and G-functions respectively, compared with 1.87 and 1.90 in **Table 4**.

Table 5 Best Fit Values of R_c for Test Stages Assuming Constant Soil Thermal Conductivity

		Line Source; λ_g=2.6 W/mK		G-function; λ_g=2.4 W/mK	
		R_c	RMSE (for Stage)	R_c	RMSE (for Stage)
Stage 2	Heat Injection	0.074	0.19	0.075	0.36
Stage 3	Recovery	0	0.24	0.06875	0.30
Stage 4	Heat Extraction	0.068	0.59	0.09375	0.61
Stage 5	Recovery	0.102	1.00	0.09375	1.10
Stage 6	Heat Injection	0.097	1.02	0.1	0.99
Stage 7	Heat Extraction	0.142	1.56	0.15625	1.66
Stage 8	Heat Injection	0.068	0.70	0.06875	0.69
Stage 9	Heat Extraction	0.213	4.04	0.325	3.60

Figure 13 Superposition Fit of Line Source and G-function Models to All Test Stages using Variable R_c (refer to Table 5 for values of R_c)

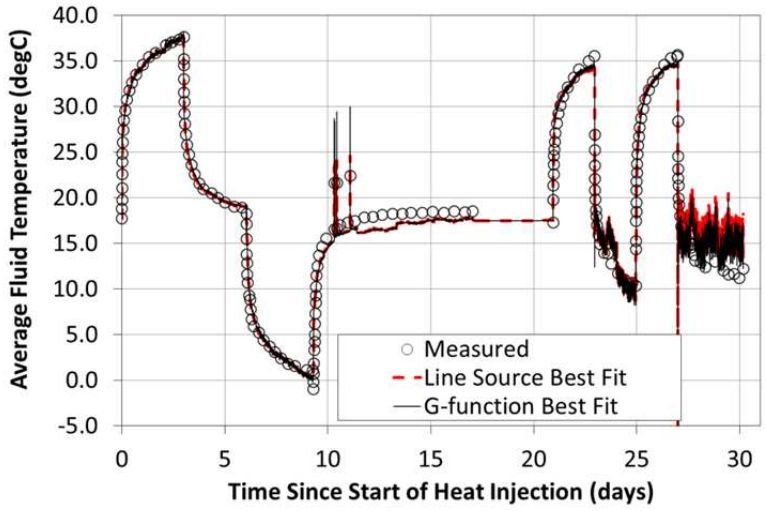

There is some merit in the hypothesis that when the pile is cooled it starts to contract and that this introduces an additional contact resistance at the pile soil boundary. This is clearly not a full explanation for the observed behaviour as it does not deal with the initial loss of fit during Stages 4 and 5 which appears unrelated to a contraction of the pile. There is also still a decline in the closeness of fit throughout the test, which suggests that there are some additional mechanisms occurring in practice which cannot be capture by the current models. Nonetheless, the results of this test do have implications for both thermal response testing (which normally only includes a single heat injection stage) and routine analysis and design (that assumes constant parameters throughout the design life of a system).

6.3 Length of Thermal response Tests

The longer a thermal response test lasts the more it costs. Consequently, the topic of test length has been variously debated for many years with respect to borehole heat exchangers [e.g 11, 16, 50, 51], with the consensus being that tests should be at least 50 hours in length. For pile heat exchangers the larger diameters and additional thermal inertia of the concrete volumes means these recommendations must be re-visited. **Figure 14** plots the change in calculated thermal conductivity and thermal resistance with time for Stage 2 of the test

based on direct analysis of the data. In both cases the analysis is carried out for a constant "start time", gradually increasing the amount of data included as the test proceeds. When using the line source model the analysis starts at approximately 27 hours, after the initial data have been discarded (refer to Section 4.1), while when using the G-function approach the test data can be used immediately from commencement of the test. Similar results to **Figure 14** can also be obtained by superposition.

Figure 14a shows the calculated thermal conductivity. For the line source model convergence of the calculated value occurs only after 60 hours or more. This implies that the test must be run for at least this duration to obtain a reliable result. The fluctuation in thermal conductivity during the test can be as much as ±20% and is probably caused by the sensitivity of the line source model to non-steady heat input to the ground (e.g. due to power fluctuations or other external influences). On the other hand, the calculations made using the G-functions tend to be stable within ±5% from 24 hours or less. This shows that the G-functions are less sensitive to small change in the gradient of the measured data and this provide greater confidence in the calculated thermal conductivity. They can also potentially be used with shorter duration tests, which would bring economic benefits. The line source model, however, is shown to require at least 72 hours of data to obtain stable results for a 300mm diameter pile. Otherwise there is a risk that the length of time of the test may significantly affect the results obtained. This figure of 72 hours should of course not be taken as universal for piles of this size as the length of time for the test results to stabilise will depend on the grout thermal conductivity and thermal diffusivity. It may be typical of cementitous materials, but lower diffusivity materials, such as bentonite grouts, may require longer test durations [42].

The variation in calculated thermal resistance with time is shown in **Figure 14b**. Surprisingly R_b, which is generally considered to be determined with less accuracy from thermal response tests [14, 22], shows only a small percentage variation, generally within ±15% for the line source case. For the G-function analysis, the results are very stable with variation of less than 1% after the first few hours

Figure 14 Change in Calculated Thermal Properties with Time (Stage 2): a) Thermal Conductivity; b) Pile Thermal Resistance

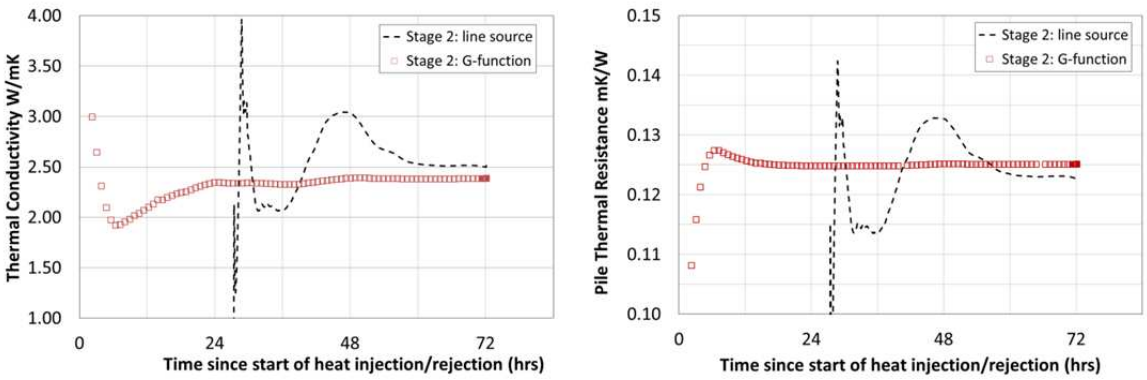

6.4 What Values of the System Characteristics should be Used?

The preceding sections present a number of analyses, more than could be conducted on a routine basis. The calculated thermal conductivity and thermal resistance values presented in **Tables 3, 4 & 5** and **Figure 14** cover a surprisingly large range. This relates to the various ways in which the real conditions differ from the idealised assumptions that must be made to practically analyses the data. Probably the most important factor in this context is the potential for changes in the value of thermal resistance (Section 6.2). However, other factors also affect the accuracy of the results, including the ambient air temperature, which cause the fluctuations of λ_g and R_b with time (Figure 14), and the length of the heat exchanger, which is not accounted for in the line source model and therefore results in over estimation of the λ_g. It is also clear that some damping of the variable applied thermal load occurs within the heat transfer pipes and fluid, and that this may need to be included within the G-function model.

In this context it is suggested that the thermal characteristics are determined from the first test stage. This would suggest λ_g = 2.4 W/mK ± 10% and R_b = 0.125 mK/W ± 10% based on the G-function model. It is important to include some indication of the expected accuracy of the results and remember that small values of statistical error associated with the model fit do not equate to an exact answer. However, it should also be stressed that the R_b value takes no account of contact resistances and that these may increase the overall resistance. In service the pile will be subjected to heating and cooling cycles so the change in contact resistance will be important for these multiple heating and cooling pulses. This point clearly needs to be the subject of further research as it could potentially have a large impact of system analysis and design.

7 Conclusions & Recommendations

A multi-stage thermal response test was carried out on a 300mm diameter test pile over the course of a month and the results analysed using both a traditional line source model and pile and concrete G-function. Two approaches were adopted, the first assuming constant thermal power and the second applying parameter estimation using superposition of variable thermal power. The results of the analysis showed that:

1. For the pile tested there is only a small difference between the two models. This is because the pile is of small diameter, larger aspect ratio (AR=87) and has a thermal conductivity similar to that of the ground.
2. While the line source model is simple to apply, it may overestimate the ground thermal conductivity by 5 to 10 % compared with the G-function models. This is due to axial effects not considered by the line source model. While the G-functions appear more complicated, they can be implemented directly in routine software with little additional effort.
3. The application of power superposition proved to be a useful approach for addressing medium term power variations and allows analysis of multiple test stages. However when used with both the line source and G-function models it overestimated the very short term fluctuations in temperature.
4. The analysis of recovery data may be better carried out using superposition of thermal power, rather than direct application of the line source model.
5. For the pile tested the calculated thermal properties obtained using the line source model required at least 72 hours to stabilise. This is because the line source model is sensitive to small changes in the measured temperature gradient and hence the precise portion of the data set which is analysed. It should be noted that lower conductivity and diffusivity piles would require longer timescales. This problem does not occur when using the G-functions, suggesting that this model is more reliable for short duration thermal response tests on piles.
6. Hysteresis was observed between the heat injection and heat rejection cycles at the end of the test. This suggests that the effective pile thermal resistance may not be constant. It is hypothesised that this effect is the result of increased contact resistance at the pile-soil boundary when the pile is cooled. However, this cannot explain all the observed behaviours. Further research is needed to confirm this hypothesis, and fully explain the observations, but if correct this will have a significant impact on long term performance as the reduced contact (increased resistance) appears to remain in place. Real piles also undergo many cycles of heating and cooling which could effect and change this contact resistance.

On this basis the following recommendations are made:

1. Pile and concrete G-functions provide an alternative method of TRT interpretation which is well suited to piles of larger diameter and smaller aspect ratios. They are also appropriate for use with shorter duration tests.
2. While the line source model can be applied for the smallest diameter piles with larger aspect ratios, it has several disadvantages. These include the requirement to discard part of the dataset, the potential to overestimate the ground thermal conductivity, and the requirement for longer test durations.
3. Owing to the potential for hysteresis, while single stage thermal response tests are recommended for the basic system characteristics, if the true system behaviour is to be understood multi-stage tests may

be required. Given the cyclic nature of real thermal loadings this may be of significant importance for fully understanding long term system behaviour.

Acknowledgements

The authors would like to thank Concept Consultants Ltd, Marton Geotechnical Services Ltd and Gecco$_2$ Ltd for their roles in construction of the test pile and carrying out the thermal response test. The work of Jasmine Low (University of Southampton) and Echo Ouyang (University of Cambridge) in the installation are also gratefully acknowledged. The lead author was funded by the Engineering and Physical Sciences Research Council (research grant number EP/H049010/1).

References

[1] Omer A. M. (2008) Ground-source heat pumps systems and applications, Renew. & Sustain. Energy Reviews, 12, 344–71.

[2] NHBC (2010) Efficient design of piled foundations for low rise housing, National House Building Council, Amersham, UK.

[3] Laloui, L. & Di Donna, A. (2011) Understanding the behaviour of energy geo-structures, Proc. Inst. Civil. Eng., 164, 184–191.

[4] He, M. M. & Lam, H. N. (2006) Study of geothermal seasonal cooling storage system with energy piles. In: Proc. ECOSTOCK Conference, Atlanta City, NJ, USA, 2006. Available at: https://intraweb.stockton.edu/eyos/energy_studies/content/docs/FINAL_PAPERS/11A-2.pdf Accessed 6 June 2013.

[5] Brandl. H. (1998) Energy piles and diaphragm walls for heat transfer from and into the ground. In: Van Impe & Haegemans (eds), Deep foundations and auger piles, Balkema, Rotterdam, pp37–60.

[6] Loveridge, F. & Powrie, W. (2013) Pile heat exchangers: thermal behaviour and interactions, Proceedings of the Institution of Civil Engineers Geotechnical Engineering, 166 (2), 178 – 196.

[7] Loveridge, F. & Powrie, W. (2014) 2D thermal resistance of pile heat exchangers, Geothermics, 50, 122 – 135.

[8] SIA (2005) Utilisation de la chaleur du sol par des ouvrages de foundation et de soutenement en beton, Swiss Associations for Engineers and Architects, Zurich.

[9] Loveridge, F. & Powrie, W. (2013) Temperature response functions (G-functions) for single pile heat exchangers, *Energy*, 57, 554 - 564.

[10] Mogensen, P/ (1983) Fluid to Duct Wall Heat Transfer in Duct System Heat Storages. Proc. Int. Conf. On Subsurface Heat Storage in Theory and Practice, Sweden, June 6 – 8, 1983, 652 – 657.

[11] Gehlin, S. (1998) Thermal response test – in situ measurement of thermal properties in hard rock, Licentiate Thesis, Lulea Technical University.

[12] Austin III, W. A. (1998) Development of an in situ system for measuring ground thermal properties. MSc Thesis, Oklahoma State University.

[13] Signorelli, S., Bassetti, S., Pahud, D. & Kohl, T. (2007), Numerical evaluation of thermal response tests, Geothermics, 36, 141-166.

[14] Witte, H. J. L. (2013) Error analysis of thermal response tests, Energy, doi:10.1016/j.apenergy.2012.11.060.

[15] IGSHPA (2007) Closed-loop/geothermal heat pump systems: Design and installation standards, International Ground Source Heat Pump Association/Oklahoma State University..

[16] Sanner, B., Hellstrom, G., Spitler, J. & Gehlin S. E. A. (2005) Thermal Response Test – Current Status and World-Wide Application, In: Proceedings World Geothermal Congress, 24-29th April 2005 Antalya, Turkey. International Geothermal Association.

[17] GSHPA (2011). Closed-loop Vertical Borehole Design, Installation & Materials Standards Issue 1.0, September 2011. Ground Source Heat Pump Association, Milton Keynes, UK.

[18] Carslaw, H. S. & Jaeger, J. C. (1959) Conduction of Heat in Solids. Second Edition, Oxford University Press.

[19] Hellstrom, G. (1991) Ground Heat Storage, Thermal Analysis of Duct Storage Systems, Theory, Department of Mathematical Physics, University of Lund, Sweden.

[20] Gehlin, S. (2002) Thermal response test, model development and evaluation, Doctoral Thesis, Lulea Technical University.

[21] Banks, D., Withers, J. G., Cashmore, G. & Dimelow, C. (2013) An overview of the results of 61 in situ thermal response tests in the UK, Quarterly Journal of Engineering Geology and Hydrogeology, 46, 281-291.

[22]Javed, S. & Fahlen, P. (2011) Thermal response testing of a multiple borehole ground heat exchanger, Int. J. of Low Carbon Technol., 6, 141 – 148.

[23] Zervantonakis, I.K. and Reuss, M., (2006) Quality requirements of a thermal response test. Proc. 10th Int. Conference on Thermal Energy Storage, Ecostock 06 , Richard Stockton College, New Jersey, USA, 31 May– 2 June 2006.

[24] Ingersoll, L. R., Zobel, O. J. & Ingersoll, A. C. (1954) Heat Conduction with Engineering and Geological Applications. 3rd Edition, New York, McGraw-Hill.

[25] Bernier, M. (2001) Ground Coupled Heat Pump System Simulation, ASHRAE Transactions, 107 (1), 605-616:

[26] Fujii, H., Okubo, H., Nishi, K., Itoi, R., Ohyama, K. & Shibata K (2009) An improved thermal response test for U-tube ground heat exchanger based on optical fiber thermometers, Geothermics, 38 (4), 399–406.

[27] Sass; I: & Lehr, C. (2011) Improvements on the thermal response test evaluation applying the cylinder source theory. In: Proceedings 36th workshop on geothermal reservoir engineering, Stanford University, Stanford, California, January 31 - February 2, 2011.

[28] Yu, X., Zhang, Y., Deng, N., Wang, J., Zhang, D. & Wang, J. (2013) Thermal response test and numerical analysis based on two models for ground-source heat pump system, Energy and Buildings, 66, 657 – 666.

[29] Loveridge, F. (2012) The thermal performance of foundation piles used as heat exchangers in ground energy systems, Doctoral Thesis, University of Southampton.

[30] Javed, S., Nakos, H. & Claesson, J. (2012) A method to evaluate thermal response tests on groundwater filled boreholes, ASHRAE Transactions, 118 (1), 540 – 549.

[31] ASHRAE (2007) ASHRAE Handbook - Heating, Ventilating, and Air-Conditioning Applications, American Society of Heating, Refrigeration and Air-Conditioning Engineers, Atlanta, 2007.

[32] Sauer, M. (2013) Evaluating improper response test data by using superposition of line source approximation, Proceedings of the European Geothermal Congress 2013, 3 – 7 June, Pisa, Italy.

[33] Javed, S. & Claesson, J. (2011) New analytical and numerical solutions for the short time analysis of vertical ground heat exchangers, ASHRAE Transactions, 117 (1), 13 – 21.

[34] Oak Ridge National Laboratory, Geothermal or ground source heat pumps, http://www.ornl.gov/sci/ees/etsd/btric/ground-source.shtml. Accessed 7th June 2013.

[35] Shonder, J. A., & Beck, J. V. (2000) A new method to determine the thermal properties of soil formations form in situ field tests, Oak Ridge National Laboratory, Report ORN/TM-2000/97, Oak Ridge, Tennessee. http://www.ornl.gov/sci/ees/etsd/btric/pdfs/com_soilproperties.pdf. Accessed 7th June 2013.

[36] Hemmingway, P. & Long, M. (2013) Energy piles: site investigation and analysis, Proc. Inst. Civil. Eng. Geotechnical Engineering, 166(6), 561-575.

[37] Austin, W., Yavuzturk, C. & Spitler, J. D. (2000) Development of an in situ system for measuring ground thermal properties, ASHRAE Transactions, 106 (1), 365 – 379.

[38] Lennon, D. J., Watt, E. & Suckling, T. P. (2009) Energy piles in Scotland, Presented at the International Conference on Deep Foundations on Bored and Auger Piles, Frankfurt, 15 May 2009.

[39] Wood, C. J., Liu, H. & Riffat, S. B. (2010) Comparison of a modelled and field tested piled ground heat exchanger system for a residential building and the simulated effect of assisted ground heat recharge, International Journal of Low Carbon Technologies, 5, 137-143.

[40]Brettman, T. P. E., Amis, T. & Kapps, M. (2010) Thermal conductivity analysis of geothermal energy piles, In: Proceedings of the Geotechnical Challenges in Urban Regeneration Conference, London UK, 26 – 28 May 2010.

[41] Park, H., Lee, S-R., Yoon, S. & Choi, J-C. (2013) Evaluation of thermal response and performance of PHC energy pile: Field experiments and numerical simulation, Applied Energy, 103, 12 – 24.

[42] Loveridge, F., Brettman, T., Olgun, C. G. & Powrie, W. (2014) Assessing the applicability of thermal response testing to energy piles, In Proc: Global Perspectives on the Sustainable Execution of Foundations Works, 21-23 May, Stockholm, Sweden.

[43] Bouazza, A., Wang, B. & Singh, R. M. (2013) Soil effective thermal conductivity from energy pile thermal tests, In: Manassero et al (Eds.) Coupled Phenomena in Environmental Geotechnics, Proceedings of the International Symposium, ISSMGE TC 215, Torino, Italy, 1-3 July 2013, Taylor & Francis, London, 211-219.

[44] Kavanaugh, S. P., Xie, L. & Martin, C. (2001) Investigation of methods for determining soil and rock formation thermal properties from short-term field tests, ASHRAE 1118-TRP

[45] Javed, S., Claesson, J. & Beier, R. A. (2011) Recovery times after thermal response tests on vertical borehole heat exchangers, Proc. 23rd IIR Int. Congress of Refrigeration (ICR2011), Prague, Czech Republic.

[46] Gnielinski, V. (1976). New equation for heat and mass transfer in turbulent pipe and channel flow, International Chemical Engineering, 16, 359 – 368.

[47] Yang, W., Shi, M., Liu, G. & Chen, Z. (2009). A two region simulation model of vertical U-tube ground heat exchangers and its experimental validation, Applied Energy, 86, 2005-2012.

[48] Yavuzturk, C. & Spitler, J. (2001). Field validation of a short timestep model for vertical ground loop heat exchangers, ASHRA Transactions, 107(1), 617-625.

[49] Raymond, J., Therrien, R., Gosselin, L. & Lefebrve, R. (2011). A review of thermal response test analysis using pump test concepts, Groundwater, 49 (6), 932 – 945.

[50] Beier, R. A. & Smith, M. D. (2003) Minimum Duration of In situ tests on Vertical Boreholes, ASHRAE Transactions, 109 (2), 475-486.

[51] Spitler, J. D., Rees, S. & Yavuzturk, C (1999) More Comments on In-situ Borehole Thermal Conductivity Testing, The Source, 12 (2) March-April 1999, 4-6. http://www.hvac.okstate.edu/research/Documents/Spitler,%20Rees,%20and%20Yavuzuturk1999.pdf. Accessed 16th July 2013.